Determining an *n*-qubit state by a single apparatus through a pairwise interaction

Hengyan Wang,[1] Wenqiang Zheng,[1] Yafei Yu,[2] Min Jiang,[1] Xinhua Peng,[1,3,*] and Jiangfeng Du[1,3]

[1]*Hefei National Laboratory for Physical Sciences at Microscale and Department of Modern Physics, University of Science and Technology of China, Hefei, Anhui 230026, China*

[2]*Laboratory of Nanophotonic Functional Materials and Devices, LQIT & SIPSE, South China Normal University, Guangzhou 510006, China*

[3]*Synergetic Innovation Center of Quantum Information & Quantum Physics, University of Science and Technology of China, Hefei, Anhui 230026, China*

(Received 17 December 2013; published 3 March 2014)

This paper shows how one can reconstruct an unknown n-qubit state by only a single apparatus. Its core is a redistribution of the information within an extended Hilbert space by coupling the unknown system with an assistant system through *only a pairwise interaction*, which results in a one-to-one mapping between the unknown density matrix elements and the probabilities of the occurrence of the eigenvalues of a single, factorized observable of the composite system. In such an interaction configuration, which is more feasible in experiments, the quality of the measurement only depends on that of the subsystem consisting a of one-qubit system coupled to a one-qubit assistant. We analyze in detail the performance of this procedure and experimentally implement it for reconstructing an unknown two-qubit state using a four-nuclear-spin system.

DOI: 10.1103/PhysRevA.89.032103 PACS number(s): 03.65.Wj, 03.67.Lx, 03.65.Ta, 76.60.−k

I. INTRODUCTION

In quantum mechanics, the state of a quantum system can be completely described by a density matrix. The results of any measurement of the quantum system can be predicted from the density matrix. Conversely, the information carried by the density matrix can be extracted with measurement. Usually the process of reconstructing an unknown quantum state by measurement is called quantum state tomography (QST) [1]. In the last several decades, different QST schemes have been presented including standard QST [2,3], QST by means of a single apparatus [4–7], QST on symmetric informationally complete positive-operator valued measure [8–12], QST on mutually unbiased bases [13–15], QST via unambiguous state discrimination [16], direct QST via weak measurement [17,18], QST via compressed sensing [19,20], and self-calibrating tomography [21–25].

The principle of complementarity proposed by Bohr [26] points out the issue that the measurements of certain noncommuting observables are needed to determine a complete quantum state. Explicitly, for an N-dimensional quantum system, N^2-1 parameters are required to determine its density matrix. Measuring an observable of this quantum system can give at most $N-1$ independent parameters. So one has to perform at least $N+1$ measurements with noncommuting observables to completely reconstructing the unknown density matrix. The simplest example is to determine the state of a spin-1/2 particle. Its density operator can be written in the form $\hat{\rho}=\frac{1}{2}\sum_{i=0}^{3} p_i\hat{\sigma}_i$, where the operators $\hat{\sigma}_i \in \{\hat{1},\hat{\sigma}_x,\hat{\sigma}_y,\hat{\sigma}_z\}$, $\hat{\sigma}_\alpha$ ($\alpha = x$, y, or z) are the Pauli operators, and $\hat{1}$ is a 2×2 unit operator. Due to the normalization condition and the traceless property of Pauli operators, one has always $p_0=1$. The standard QST method consists of respectively measuring the spin components along the x, y, and z axes. By doing this, all of p_i can be obtained by $\mathrm{Tr}(\hat{\rho}\hat{\sigma}_i)$, which means that we get the complete information of the quantum state.

In this paper, we focus on another method for QST by repeated measurements of a single observable. One practical advantage of QST with a single observable is that it avoids some experimental uncertainties related to measurement setups for incompatible observables [4–6,27,28]. An overview on quantum state tomography with a single observable is given in Ref. [28]. The main idea is to redistribute the information about the unknown quantum state into an extended system by introducing an assistant system A whose dimension of Hilbert space is no less than the the system S, and a one-to-one mapping is thus generated between the unknown density matrix $\hat{\rho}$ and the joint probabilities to observe a single observable. This can be done by either measuring a single "universal" observable on an extended Hilbert space [29] or measuring a single, factorized observable if we first let the system S interact with the assistant A for some time under a suitable, interactional measurement Hamiltonian [4]. For the latter case, Allahverdyan *et al.* [4] determined the condition which the optimized measurement Hamiltonian should meet for the best determination of a two-level quantum system. In Ref. [5], we studied in detail this type of measurement under a Heisenberg coupling Hamiltonian and we found the optimized measurement Hamiltonian for the simplest case, i.e., a one-qubit system coupled to a one-qubit auxiliary system. We also experimentally demonstrated it using a nuclear spin 1/2 as the system and a different nuclear spin 1/2 as the assistant. Recently, we considered the case of a high-dimensional quantum system and obtained the condition for the best determination [6]. However, it is both theoretically and experimentally difficult to achieve the optimal measurement Hamiltonian for the best determination for a many-qubit system.

In this paper, we generalize the previous results on the two-level system to an n-qubit system, where the system S interacts with the assistant A by *only a pairwise interaction*. Such a simple Hamiltonian is feasible for the optimal measurement, which overcomes both the theoretical and experimental

*xhpeng@ustc.edu.cn

difficulties considered in the previous research, at the price of a small loss of the quality of the measurement. We study the details of this procedure. As an experimental example, we present the results of the reconstruction of the density matrix of a two-qubit nuclear spin system in a four-nuclear-spin system, where we consider three cases: the unknown quantum system was initially prepared in a mixed state, a pseudo-pure product state, and a pseudo-entangled pure state.

II. PRINCIPLE AND GENERALIZATION

Consider a large but finite number of identical quantum systems S consisting of n spin-1/2 particles whose state can be represented by

$$\hat{\rho}_S = \frac{1}{2^n}\sum_{s=0}^{4^n-1} c_s \hat{B}_s, \tag{1}$$

where a complete set of base operators $\{\hat{B}_s\}$ consists of 4^n product operators $\hat{B}_s$:

$$\hat{B}_s = \prod_{k=1}^{n} \hat{\sigma}_i^k, \quad 0 \leqslant s \leqslant 4^n - 1. \tag{2}$$

Here n is the total number of spins in the system under consideration, k is an index for the spin and $i \in \{0,1,2,3\}$, corresponding to the unit operator and Pauli operators $(\{\hat{1},\hat{\sigma}_x,\hat{\sigma}_y,\hat{\sigma}_z\})$. s is the quaternary string constituted by all of i, covering from $00\ldots00$ to $33\ldots33$. The operators $\{\hat{B}_s\}$ satisfy

$$\mathrm{Tr}(\hat{B}_s\hat{B}_r) = 2^n\delta_{sr}, \tag{3}$$

where Tr is the trace operation and the Kronecker delta $\delta_{sr} = 1$ when $s = r$, otherwise 0. To determine the state $\hat{\rho}_S$, we can measure the vector $\vec{c} = \mathrm{Tr}(\vec{\hat{B}}\hat{\rho}_S) = (c_0, c_1, \ldots, c_{4^n-1})^T$ with $\vec{\hat{B}} = (\hat{B}_0, \hat{B}_1, \ldots, \hat{B}_{4^n-1})^T$. Note that $\hat{B}_0 = \hat{1}^{\otimes n}$ is a $2^n \times 2^n$ unit operator and $c_0 = 1$ due to the normalization condition $\mathrm{Tr}(\hat{\rho}_S) = 1$. This procedure generally refers to the standard QST, which involves $N+1$ noncommuting observables.

Alternatively, all the c_s can also be obtained through QST with a single measurement apparatus by interacting the unknown system S with an assistant system A in a known state [4,5]. The dimension of the assistant system A must be no less than N. The composite system $S + A$ is initially in a product state $\hat{\rho}_0^{S+A} = \hat{\rho}_S \otimes \hat{\rho}_A$, and then the interaction between them drives the system into an entangled state $\hat{\rho}_\tau = \hat{U}(\tau)\hat{\rho}_0^{S+A}\hat{U}^\dagger(\tau)$ after a duration τ, where the propagator $\hat{U}(\tau) = e^{-i\hat{H}\tau}$ with the interaction Hamiltonian $\hat{H}$ between S and A. The information of the unknown system S is redistributed on the whole Hilbert space of the combined system. Therefore, we can choose to measure a single, factorized observable $\hat{P} = \hat{\omega}^{(S)} \otimes \hat{o}^{(A)}$ on the combined system to determine the unknown state $\hat{\rho}_S$, where $\hat{\omega}^{(S)}$ is pertaining to S and $\hat{o}^{(A)}$ pertaining to A. Without loss of generality, the observables $\hat{\omega}^{(S)}$ and $\hat{o}^{(A)}$ to be measured can be their x components.

Then the jointed projectors $\hat{P}_q = \hat{P}_{ij} = \hat{\omega}_i^{(S)} \otimes \hat{o}_j^{(A)}$ are

$$\hat{P}_q = \frac{1}{2^{2n}} \prod_{\otimes l=1}^{2n} [\hat{1} + (-1)^{h_l}\hat{\sigma}_x^l], \tag{4}$$

where h_l takes 0 or 1, $q = h_{2n}\ldots h_1h_0$ ranging from $00\ldots00$ to $11\ldots11$. There are totally 4^n projectors covering all of the measurement outcomes. The repeated measurements of the observable $\hat{P}$ give the complete set of the jointed probabilities p_q,

$$p_q = \mathrm{Tr}\left(\hat{P}_q\hat{U}\rho_0^{S+A}\hat{U}^\dagger\right) = \mathrm{Tr}(\hat{P}_q\hat{U}\hat{\rho}_S \otimes \hat{\rho}_A\hat{U}^\dagger). \tag{5}$$

As a result of Eq. (1), Eq. (5) can be written in the form

$$p_q = \frac{1}{2^n}\sum_{j=0}^{4^n-1} c_s\,\mathrm{Tr}[\hat{P}_q\hat{U}(\hat{B}_s \otimes \hat{\rho}_A)\hat{U}^\dagger]. \tag{6}$$

To determine the quantum state, we need the $4^n - 1$ unknown coefficients c_s which are related to the probabilities p_q by a transfer matrix $\mathcal{M}$:

$$\mathcal{M} \times \frac{1}{2^n}\begin{pmatrix} c_0 \\ c_1 \\ c_2 \\ \vdots \\ c_{4^n-1} \end{pmatrix} = \begin{pmatrix} p_0 \\ p_1 \\ p_2 \\ \vdots \\ p_{4^n-1} \end{pmatrix}. \tag{7}$$

The elements of linear mapping $\mathcal{M}$ are determined by

$$\mathcal{M}_{qs} = \mathrm{Tr}[\hat{P}_q\hat{U}(\hat{B}_s \otimes \hat{\rho}_A)\hat{U}^\dagger], \quad 0 \leqslant q,s \leqslant 4^n - 1. \tag{8}$$

Therefore, if the determinant Δ of the transfer matrix $\mathcal{M}$ is not zero, we can obtain the vector $\vec{c} = (c_0, c_1, \ldots, c_{4^n-1})^T$ (i.e., the unknown state $\hat{\rho}_S$) by the joint probabilities $\vec{p} = (p_0, p_1, \ldots, p_{4^n-1})^T$. The precision of the back-calculation depends on the size of the determinant $|\Delta|$ of $\mathcal{M}$, roughly $\propto 1/|\Delta|$. Maximizing $|\Delta|$ will minimize the statistical error of the estimation during the inversion of Eq. (7). Therefore, the best determination requires us to maximize $|\Delta|$ by a suitable choice of the initial condition of the assistant $\hat{\rho}_A$ and the propagator $\hat{U}(\tau)$ (i.e., the interaction Hamiltonian $\hat{H}$ and the duration τ). Reference [4] analytically gives the maximal value of $|\Delta|$ and the detailed form of $\hat{U}(\tau)$ for a two-level system S when the assistant A is initially in a pure state $\hat{\rho}_A = \frac{1}{2}(\hat{1} + \hat{\sigma}_z^A)$ or a completely disordered state $\hat{\rho}_A = \frac{1}{2}\hat{1}$. Although we obtained the maximal value of $|\Delta|$ for an N-dimensional quantum system [6], it is difficult to obtain the detailed form of $\hat{U}(\tau)$ to achieve this maximum. The optimal evolution $\hat{U}(\tau)$ can be numerically searched in a $2N \times 2N$ Hilbert space by optimal control method. Obviously this is a substantial task.

A simple and effective method can be obtained if we introduce a *pairwise interaction* between the system S and the assistant A:

$$\hat{H} = \sum_{k=1}^{n} \hat{H}^{(k,k_a)}, \tag{9}$$

as shown in Fig. 1. Here k and k_a, respectively, represent the kth qubits of S and A. The evolution propagator $\hat{U}(\tau)$ under the interaction Hamiltonian $\hat{H}$ after a time τ can be written as

$$\hat{U}(\tau) = \prod_{\otimes,k=1}^{n} \hat{U}^{(k,k_a)}(\tau), \tag{10}$$

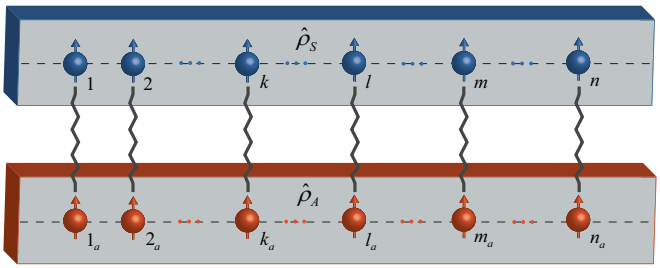

FIG. 1. (Color online) Schematic diagram for measuring an n-qubit unknown state by a single observable through a *pairwise interaction*. The upper spin chain consisting of qubits $1,2,\ldots,n$ is the unknown system S, while the lower chain consisting of qubits $1_a,2_a,\ldots,n_a$ is the assistant A. The solid lines represent the *pairwise interactions* between qubit k and k_a.

where $\hat{U}^{(k,k_a)}(\tau)=e^{-i\hat{H}^{(k,k_a)}\tau}$ pertaining to the subspace spanned by qubit k and its corresponding assistant qubit k_a. If the assistant state $\hat{\rho}_A$ has the factorable form $\hat{\rho}_A=\prod_{\otimes,k=1}^{n}\hat{\rho}_A^{(k)}$, it is straightforward to find from Eq. (8) that the transfer matrix $\mathcal{M}$ has a simple form:

$$\mathcal{M}=\prod_{\otimes,k=1}^{n}\tilde{\mathcal{M}}^{(k,k_a)}, \tag{11}$$

where $\tilde{\mathcal{M}}^{(k,k_a)}$ is the transfer matrix of the subspace spanned by qubits k and k_a. Moreover, if the states of all the qubits of A are equivalent, $\tilde{\mathcal{M}}^{(k,k_a)}$ for each pair of qubits k and k_a are the same. Then we have the determinant of $\mathcal{M}$,

$$\Delta=\det(\mathcal{M})=\det(\tilde{\mathcal{M}}^{(k,k_a)})^{n\times 4^{(n-1)}}. \tag{12}$$

It shows that the maximization of $|\Delta|$ in a $2n$-qubit system under such a *pairwise* interaction configuration is equivalent to the maximization of $|\det(\tilde{\mathcal{M}}^{(k,k_a)})|$ in a two-qubit system. This allows us to draw a conclusion that searching an optimal evolution $U(\tau)$ (i.e., $\hat{H}$ and τ in a $2n$-qubit system under such a configuration is reduced into searching for an optimal evolution $\hat{U}^{(k,k_a)}(\tau)$ (i.e., $\hat{H}^{(k,k_a)}$ and τ) in a two-qubit system. The *pairwise* interaction is a key prerequisite in this scheme which is experimentally feasible. Consequently, we can employ the result of a two-level quantum system [4,5] for the best determination of an n-qubit system with *pairwise* interaction. For a two-level quantum system, the maximum of $|\Delta|$ is $1/48\sqrt{3}$ for a pure assistant [4,5]. Therefore, one gets

$$|\Delta|_{max}=\left(\frac{1}{48\sqrt{3}}\right)^{n\times 4^{n-1}} \tag{13}$$

for an n-qubit system in this case. Comparing to the result of Ref. [6], the maximum of $|\Delta|$ of an $N(=2^n)$-dimension system for a general interaction Hamiltonian that involves all N^2-1 independent generators of group SU(N) is

$$\frac{1}{2^{n\times 4^n}}\sqrt{\frac{(2^n-1)^{4^n-1}}{(2^n+1)^{4^n-1}}} \tag{14}$$

which mainly lies on the factor $[1/2]^{n\times 4^n}$ when n is very large. Eq.uations (13) and (14) have a similar growth law with the size n of the system, but the present scheme [Eq. (13)] has a slightly smaller base $(\frac{1}{48\sqrt{3}})^{1/4}\sim 0.33$ than the optimal value $\sim 1/2$ for a general interaction Hamiltonian [Eq. (14)].

For a completely disordered assistant, the optimal propagator $\hat{U}(\tau)$ for a two-level quantum system [5] can be achieved with the measurement Hamiltonian

$$\hat{H}^{opt}=\sqrt{2}(\hat{I}_z^1\pm\hat{I}_z^{1a})+4\sqrt{2}\hat{I}_x^1\hat{I}_x^{1a}+2\hat{I}_z^1\hat{I}_z^{1a} \tag{15}$$

and the duration $\tau=\pi/4$. Here $\hat{I}_\alpha=\hat{\sigma}_\alpha/2$ ($\alpha=x$, y, or z). In our following demonstration experiment, we chose the completely disordered state for the assistant that is experimentally easy to prepare. In this case, the maximal size of the determinant $|\Delta|$ is $1/128$ [5].

III. EXPERIMENTAL IMPLEMENTATION

The experiments were carried out at room temperature on a Bruker AV-400 spectrometer (9.4 T). The physical system in our experiment is iodotrifluoroethylene molecules (C_2F_3I) dissolved in d-chloroform. The molecular structure and relevant parameters are shown in Fig. 2. One ^{13}C nucleus and three ^{19}F nuclei represent a four-nuclear-spin system. ^{13}C and F_1 consist of the system labeled as qubit 1 and qubit 2, respectively. F_2 and F_3 consist of the assistant labeled as qubit 1_a and qubit 2_a, respectively (see Fig. 1). The natural Hamiltonian of the four-nuclear-spin system in the double rotating frame is

$$\hat{H}_{nmr}=\sum_{i=1}^{4}\omega_i\hat{I}_z^i+2\pi\sum_{i<j}^{4}J_{ij}\hat{I}_z^i\hat{I}_z^j, \tag{16}$$

where ω_i is the chemical shift of spin i and J_{ij} is the scalar coupling strength between spins i and j. Note that $\hat{I}_z^1$, $\hat{I}_z^2$, $\hat{I}_z^3$, and $\hat{I}_z^4$ correspond to $\hat{I}_z^1$, $\hat{I}_z^{1_a}$, $\hat{I}_z^2$, and $\hat{I}_z^{2_a}$ in the diagram of the molecule (Fig. 2).

Figure 3 shows the flowchart of the experiment for measuring an unknown state by a single observable, which is divided into three parts:

(a) Initial state preparation $\hat{\rho}_S\otimes\frac{1}{4}\hat{1}$. Here in the experiments, the assistant A is initially in a completely disordered state. We verify this scheme for reconstructing various

^{13}C	$^{19}F_1$	$^{19}F_2$	$^{19}F_3$		T_2
15479.7Hz	-275.7Hz	-297.7Hz	39.1Hz	^{13}C	7.9s
	-42677.7Hz	64.6Hz	-129.0Hz	$^{19}F_1$	6.8s
		-33122.4Hz	51.5Hz	$^{19}F_2$	4.4s
			-56445.8Hz	$^{19}F_3$	4.8s

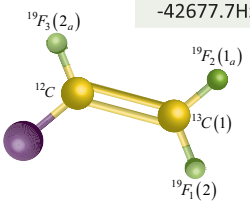

FIG. 2. (Color online) Molecular structure and relevant parameters of iodotrifluoroethylene. ^{13}C and three ^{19}F nuclei are used as a four-qubit quantum system, and the labels in brackets near the nuclei correspond to the qubits in Fig. 1. The diagonal and nondiagonal elements represent the chemical shifts and the coupling constants (in units of Hz) respectively. The spin-lattice relaxation times T_1 are 21 s for ^{13}C and 12.5 s for ^{19}F. These parameters are measured at the temperature $T=303$ K.

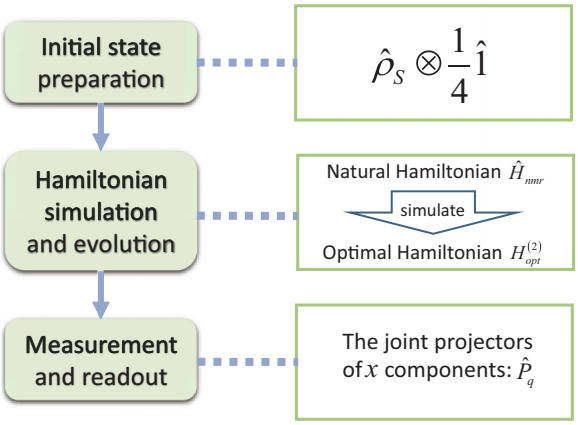

FIG. 3. (Color online) Flowchart of the experiments. The system S is initially in an unknown state $\hat{\rho}_S$ and the assistant A is initially in a completely disordered state $\frac{1}{4}\hat{1}$. Then we drive the composite system $S+A$ to evolve under an optimal Hamiltonian of Eq. (19) for a time τ which is simulated by NMR techniques. Finally we measure a single, factorable observable $\hat{P}$, i.e., their x components of Eq. (4).

quantum states $\hat{\rho}_S$ (a mixed state, a pseudo-pure state and a pseudo-entangled state).

(b) Dynamical evolution $\hat{U}(\tau) = e^{-i\hat{H}\tau}$ under the optimal interaction Hamiltonian $\hat{H}$ for the duration τ. We simulate the dynamics by nuclear magnetic resonance (NMR) techniques.

(c) Measurement of the joint probabilities p_q and then the reconstruction of the unknown quantum state by the inverse mapping.

A. Initialization

In our experiment, the assistant A is initially in a completely disordered state $\frac{1}{4}\hat{1}$ and then we test the scheme for three different cases listed in Table I: when the unknown state $\hat{\rho}_S$ is a mixed state $\hat{\rho}_{S1}$, a pseudo-pure product state $\hat{\rho}_{S2}$ and a pseudo-entangled state $\hat{\rho}_{S3}$, respectively. In NMR quantum information, we usually use the pseudo-pure state (PPS) [30] $\hat{\rho} = \frac{1-\varepsilon}{2^n}\hat{1} + \varepsilon|\psi\rangle\langle\psi|$ instead of an ideal pure state $|\psi\rangle$, where $\varepsilon \sim 10^{-5}$ is the polarization. Since unitary operations and measurement in NMR do only affect the pure state part except for a trivial scalar factor ε, a PPS is equivalent to the corresponding pure state. When $|\psi\rangle$ is an entangled state, we call the state of the system as a "pseudo-entangled state." Here we only consider the traceless deviation part $\hat{\rho}_\Delta$ of PPS $\hat{\rho} = \frac{1}{2^n}\hat{1} + \varepsilon\hat{\rho}_\Delta$ [31]. For example, for the thermal equilibrium state $\hat{\rho}_{S_1}$ of the system S, $\hat{\rho}_\Delta \propto \hat{I}_z^1 + \gamma_F/\gamma_C \hat{I}_z^2$, where γ_C and γ_F are gyromagnetic ratios of nuclei ^{13}C and ^{19}F respectively. Their ratio is $\gamma_C/\gamma_F \approx 1:3.7415$. Using the PPS technique [30,31], we prepare a pseudo-pure product state $\hat{\rho}_{S_2}$ with $\hat{\rho}_\Delta \propto \hat{I}_z^1 + \hat{I}_z^2 + 2\hat{I}_z^1\hat{I}_z^2$ corresponding to the pure state $|00\rangle_{12}$, and a pseudo-entangled state $\hat{\rho}_{S_3}$ with $\hat{\rho}_\Delta \propto 2(\hat{I}_x^1\hat{I}_x^2 - \hat{I}_y^1\hat{I}_y^2 + \hat{I}_z^1\hat{I}_z^2)$ corresponding to the entangled state (Bell state) $\frac{1}{\sqrt{2}}(|00\rangle + |11\rangle)_{12}$. The pulse sequences for the preparation are shown in Table I. With standard QST [32], we obtained the experimental fidelities of these three prepared deviation matrices $\hat{\rho}_{S1}$, $\hat{\rho}_{S2}$, and $\hat{\rho}_{S3}$, which are 0.997, 0.996, and 0.996. The fidelity is defined by [33]

$$F = \frac{\mathrm{Tr}(\hat{\rho}_{ini}\hat{\rho}_{th})}{\sqrt{\mathrm{Tr}\left(\hat{\rho}_{ini}^2\right)\mathrm{Tr}\left(\hat{\rho}_{th}^2\right)}}, \tag{17}$$

where $\hat{\rho}_{ini}$ is the experimentally reconstructed density matrix and $\hat{\rho}_{th}$ is the theoretical one.

TABLE I. (Color online) Pulse sequences for preparing the three different initial states $\hat{\rho}_S \otimes \frac{1}{4}\hat{1}$ of the composite system $S+A$. Here $[\theta]^k_{\hat{v}}$ denotes a θ rotation of qubit k around $\hat{v}$ axis, Gz represents a pulsed-field-gradient along $z-$ axis to destroy all the transverse magnetization generated by the radio frequency (rf) pulses, and the delay $d_1 = |\frac{1}{4J_{12}}|$ is a free evolution under natural Hamiltonian $\hat{H}_{nmr}$ with the duration d_1. Here we used spatial averaging method [30,34] to prepare a PPS. Based on PPS, we prepared a pseudo-entangled state with a pseudo-Hadamard gate and controlled-NOT gate (CNOT) [35]. CNOT(12) denotes that qubit 1 is a controlled qubit while qubit 2 is a target qubit.

$\hat{\rho}_S$	$\hat{\rho}_\Delta$	Pulse sequence
$\hat{\rho}_{S1}$	$\hat{I}_z^1 + 3.7415\hat{I}_z^2$	$\left[\frac{\pi}{2}\right]_x^{1_a,2_a} - Gz$
$\hat{\rho}_{S2}$	$\hat{I}_z^1 + \hat{I}_z^2 + 2\hat{I}_z^1\hat{I}_z^2$	$[0.3205\pi]_x^2\left[\frac{\pi}{2}\right]_x^{1_a,2_a} - Gz - [\pi]_y^1\left[\frac{\pi}{4}\right]_{-x}^2 - d_1 - [\pi]_y^{1,2} - d_1 - \left[\frac{5\pi}{4}\right]_y^2 - Gz$
$\hat{\rho}_{S3}$	$2\left(\hat{I}_x^1\hat{I}_x^2 - \hat{I}_y^1\hat{I}_y^2 + \hat{I}_z^1\hat{I}_z^2\right)$	$PPS - \left[\frac{\pi}{2}\right]_y^1 - CNOT(12)$

B. Hamiltonian simulation and evolution

For a completely disordered assistant, the optimal propagator for an unknown two-bit state [5] can be

$$\hat{U}^{(2)}_{opt}(\tau) = e^{-i\hat{H}^{(2)}_{opt}\tau}, \tag{18}$$

where the optimal Hamiltonian is

$$\hat{H}^{(2)}_{opt} = \sqrt{2}\left(\hat{I}_z^1 + \hat{I}_z^2 + \hat{I}_z^{1_a} + \hat{I}_z^{2_a}\right) + 2\left(\hat{I}_z^1\hat{I}_z^{1_a} + \hat{I}_z^2\hat{I}_z^{2_a}\right) + 4\sqrt{2}\left(\hat{I}_x^1\hat{I}_x^{1_a} + \hat{I}_x^2\hat{I}_x^{2_a}\right) \tag{19}$$

and $\tau = \frac{\pi}{4}$. The optimal Hamiltonian is the Heisenberg XZ model while the natural Hamiltonian of the sample is the Ising model of Eq. (16). In general, if the different terms of Hamiltonian do not commute with each other, we cannot realize the terms sequentially. However, it is possible to approximate the overall evolution by using Trotter's formula [36,37]

$$e^{(A+B)\delta t} = e^{(A\delta t/2)}e^{(B\delta t)}e^{(A\delta t/2)} + O(\delta t^3) \tag{20}$$

if the duration δt is kept sufficiently short. Our target Hamiltonian of Eq. (19) can be decomposed into two non-commutative parts,

$$\hat{H}_x = 4\sqrt{2}\left(\hat{I}_x^1\hat{I}_x^{1_a} + \hat{I}_x^2\hat{I}_x^{2_a}\right),$$
$$\hat{H}_z = \sqrt{2}\left(\hat{I}_z^1 + \hat{I}_z^2 + \hat{I}_z^{1_a} + \hat{I}_z^{2_a}\right) + 2\left(\hat{I}_z^1\hat{I}_z^{1_a} + \hat{I}_z^2\hat{I}_z^{2_a}\right). \tag{21}$$

Then the propagator of Eq. (18) can be approximately written as

$$\hat{U}^{(2)}_{opt}(\tau) = \prod_{i=1}^{m} \hat{U}^{m}(\delta t) = \left\{ \hat{U}_z\left(\frac{\delta t}{2}\right)\hat{U}_x(\delta t)\hat{U}_z\left(\frac{\delta t}{2}\right)\right\}^m + O(\delta t^3), \quad (22)$$

where $\tau = m\delta t$ is the whole evolution time, and

$$\hat{U}_z\left(\frac{\delta t}{2}\right) = e^{-i\frac{\delta t}{2}\hat{H}_z}, \quad \hat{U}_x(\delta t) = e^{-i\delta t\hat{H}_x} \quad (23)$$

represent the evolutions under the partial Hamiltonians. Theoretically, more pieces m and shorter δt are desired for more accuracy of the approximation. However, experimentally we will choose an appropriate short time δt to make the approximation effective. If $\tau = \pi/4$ and $m = 2$, The resulting approximate evolution

$$\hat{U}^{(2)}_{ap}(\tau) = \left\{ \hat{U}_z\left(\frac{\delta t}{2}\right)\hat{U}_x(\delta t)\hat{U}_z\left(\frac{\delta t}{2}\right)\right\}^2 \quad (24)$$

has a fidelity of 0.996 with the target evolution, where the gate fidelity is defined $F(\hat{U}^{(2)}_{opt}(\tau), \hat{U}^{(2)}_{ap}(\tau)) = \mathrm{Tr}[\hat{U}^{(2)}_{ap}(\tau)^\dagger \hat{U}^{(2)}_{opt}(\tau)]/16$ [33]. The $\hat{U}_z(\frac{\delta t}{2})$ and $\hat{U}_x(\delta t)$ operators can be implemented by the free evolution and rf pulses. Figure 4 shows the pulse sequence for approximately implementing the propagator $\hat{U}^{(2)}_{ap}(\tau)$. This bottom-up approach involves a series of rf pulses and evolutions, and hence accumulates considerable experimental errors and decoherence effects. In this experiment, to improve the experimental precision, we used an alternative way to achieve the target propagator with engineered quantum control pulses [38–40]. It exploits the gradient ascent pulse engineering (GRAPE) technique to synthesize $\hat{U}^{(2)}_{opt}(\tau)$ with one single engineered rf pulse only. Thus the error accumulation due to gate imperfections is avoided, and the experimental fidelity for the target propagator is maintained at a high level. The GRAPE coherent control pulse for implementing $\hat{U}^{(2)}_{opt}(\tau)$ was theoretically obtained with a high fidelity of 0.997 and a pulse length 8 ms.

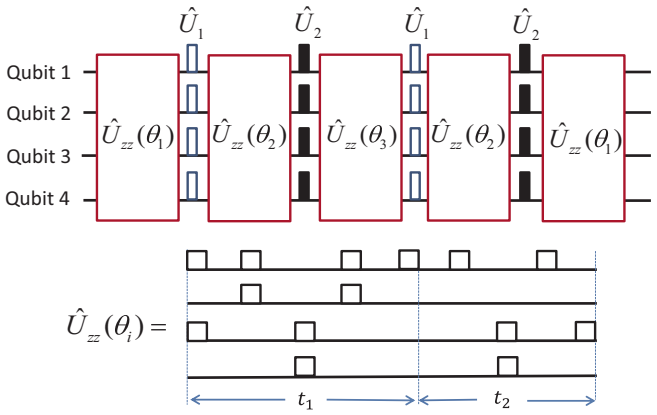

FIG. 4. (Color online) Pulse sequence for implementing the propagator $\hat{U}^{(2)}_{ap}(\tau)$. Here, $\hat{U}_{zz}(\theta_i) = e^{-i\theta_i(\hat{I}^1_z\hat{I}^{1a}_z + \hat{I}^2_z\hat{I}^{2a}_z)}$ with $\theta_3 = 2\theta_1 = 2\delta t$, $\theta_2 = 4\sqrt{2}\delta t$ and $t_1 = |\theta_i/(2\pi J_{11_a})|$, $t_2 = |\theta_i/(2\pi J_{22_a}) - \theta_i/(2\pi J_{11_a})|$. The local operators $\hat{U}_1 = e^{-i\frac{\sqrt{2}}{2}\delta t(\hat{I}^1_z+\hat{I}^2_z+\hat{I}^{1a}_z+\hat{I}^{2a}_z)}e^{-i\frac{\pi}{2}(\hat{I}^1_y+\hat{I}^2_y+\hat{I}^{1a}_y+\hat{I}^{2a}_y)}$ and $\hat{U}_2 = e^{i\frac{\pi}{2}(\hat{I}^1_y+\hat{I}^2_y+\hat{I}^{1a}_y+\hat{I}^{2a}_y)}e^{-i\frac{\sqrt{2}}{2}\delta t(\hat{I}^1_z+\hat{I}^2_z+\hat{I}^{1a}_z+\hat{I}^{2a}_z)}$.

C. Measurement and reconstruction

After the coupling evolution, we measured the x components of the four qubits to obtain the joint probabilities p_q of the projective operators $\hat{P}_q$ in Eq. (4). An equivalent choice would be the y components, while z components are infeasible due to the symmetry properties of the evolution [5]. For this purpose, we transferred the x components to z components using a $[\frac{\pi}{2}]^{1,2,1_a,2_a}_{-y}$ pulse and destroyed off-diagonal elements by a magnetic field gradient pulse G_z. The populations could then be measured by applying another reading-out pulse to each of the qubits and measuring their free induction decays (FIDs). The resulting pulse sequence for the readout is thus

$$\left[\frac{\pi}{2}\right]^{1,2,1_a,2_a}_{-y} - Gz - \mathrm{SWAP}(1j) - \left[\frac{\pi}{2}\right]^{1}_{y} - \mathrm{FID}(^{13}C), \quad (25)$$

where $j = 1$, 2, 1_a, or 2_a denotes qubit j, and SWAP$(1j)$ is SWAP gate between qubit 1 and qubit j. Because we used an unlabeled sample, the molecules with a ^{13}C nucleus are present at a concentration of about 1% (the natural abundance). The signals of ^{19}F from the quantum register with the ^{13}C nucleus are hidden under the signals from the molecules containing the ^{12}C isotope. Accordingly, the information of the ^{19}F spins is transferred to the ^{13}C spin by a SWAP gate and read through the ^{13}C spectrum. The measured FIDs after the reading-out pulses along with the normalization condition $\sum_q p_q = 1$ allows us to reconstruct 16 diagonal elements (populations) in the density matrix, which correspond to 16 joint probabilities p_q. The information about the state $\hat{\rho}_S$ was then obtained by the inverse mapping $\mathcal{M}^{-1}$.

D. Experimental results

Figure 5 shows the experimentally observed NMR signals after Fourier transformation of the corresponding FIDs for the carbon spin for three different initial states: the thermal equilibrium state $\hat{\rho}_{S1}$, the pseudo-pure state $\hat{\rho}_{S2}$, and the pseudo-entangled state $\hat{\rho}_{S3}$. Here fluorine's information (F_1, F_2, F_3) is detected through the ^{13}C NMR spectra by SWAP gates acting on ^{13}C and ^{19}F. The intensities of the different resonance lines correspond directly to population differences [41], corresponding to the joint probabilities p_q of projection operators on the x direction. We fit the NMR signals by Lorentzian curves to obtain their intensities. From these populations, we determine the initial condition c_s by inverting Eq. (7). The deduced coefficients c_s are shown in Fig. 6, and agree well with the theoretical ones. The average standard error is around 4%. To further quantify the experimental states, we calculate the state fidelities by Eq. (17). The experimental fidelities of three initial states $\hat{\rho}_{S1}$, $\hat{\rho}_{S2}$, and $\hat{\rho}_{S3}$ reconstructed by this method are 0.998, 0.995, and 0.987, respectively.

The experimental errors mainly come from the inhomogeneity of static magnetic fields, the imperfection of rf and

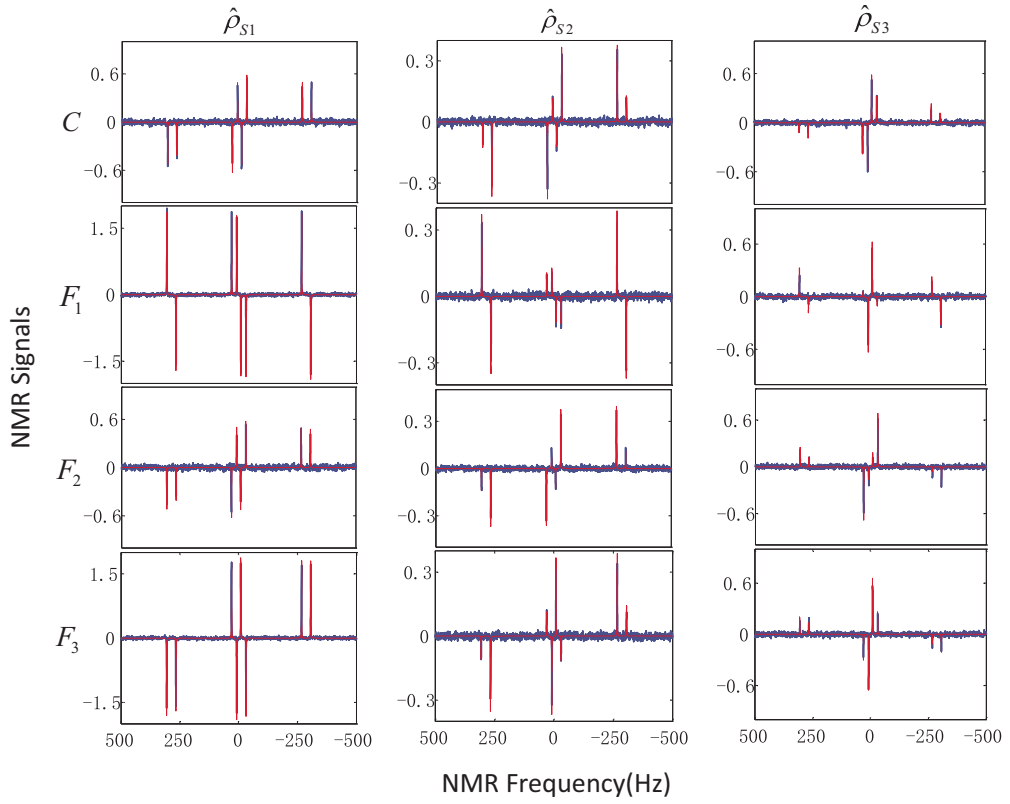

FIG. 5. (Color online) Experimental ^{13}C NMR spectra (denoted by thick blue lines) for reconstructing the three different unknown states: the thermal equilibrium state $\hat{\rho}_{S1}$, the pseudo-pure state $\hat{\rho}_{S2}$, and the pseudo-entangled state $\hat{\rho}_{S3}$ from left to right. From top to bottom are the final information of ^{13}C, F_1, F_2, and F_3 sequently. The intensities of different resonance lines correspond directly to population differences between two related energy levels. Fluorine's information is observed through the ^{13}C NMR spectra by SWAP gates acting on ^{13}C and ^{19}F. The theoretical expectations are denoted by thin red lines obtained by a NMR simulation program (NMRSIM) in Bruker's TopSpin^{TM} software package. The numbers of repeated scans for $\hat{\rho}_{S1}$, $\hat{\rho}_{S2}$ and $\hat{\rho}_{S3}$ are, respectively, 32, 32, and 64.

GRAPE pulses, and the relaxation effect. In experiments, we used 2–4 GRAPE pulses for the equilibrium state $\hat{\rho}_{S1}$, 4–5 for the pseudo-pure state $\hat{\rho}_{S2}$, and 5–6 for the pseudo-entangled state $\hat{\rho}_{S3}$. Therefore, the experimental fidelity of $\hat{\rho}_{S3}$ is relatively low compared to $\hat{\rho}_{S1}$ and $\hat{\rho}_{S2}$ due to the more complex pulse sequence. The experimental time is about 38 ms for $\hat{\rho}_{S1}$, 42 ms for $\hat{\rho}_{S2}$, and 57 ms for $\hat{\rho}_{S3}$.

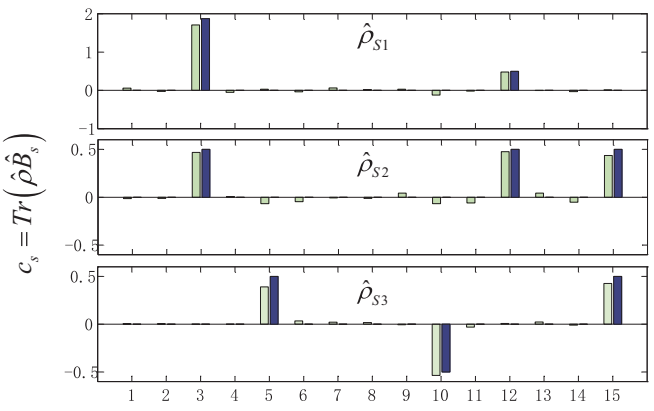

FIG. 6. (Color online) Experimentally reconstructed coefficients c_s from the experimentally measured joint probabilities p_q by the inverse mapping $\mathcal{M}^{-1}$ for three initial states $\hat{\rho}_{S1}$, $\hat{\rho}_{S2}$, and $\hat{\rho}_{S3}$. c_s is from 1 to 15 where c_0 is the coefficient of identity.

IV. CONCLUSIONS

QST with a single observable appears highly attractive since this may well have practical advantages compared with standard QST; e.g, it is more economical, more easily accessible in experiments, and the incomplete or noisy experimental data in quantum mechanical systems can be more easily dealt with using standard statistical and information theoretical methods [4]. We consider the measure scheme of an n-qubit unknown quantum state by means of a single observable, where a *pairwise* interaction is introduced as the controlled Hamiltonian to couple the unknown system with a known n-qubit assistant. Under this configuration, the quality of the measurement scheme depends on that of the subsystem consisting of two qubits; i.e., maximizing the size of the determinant $|\Delta|$ in a $2n$-qubit system is equivalent to maximizing $|\det(\tilde{\mathcal{M}}^{(k,k_a)})|$ in a two-qubit system. Therefore, the previous results can be generalized into an n-qubit case. A simple dynamical process (e.g., by a Heisenberg XZ model or a Heisenberg XY model) can afford a very valid determination of $\hat{\rho}_S$ to maximize $|\Delta|$ in such a *pairwise* interaction. This type of interaction is always found in many physical systems:

apart from nuclear spins (like in this work), they also occur in quantum dots [42–44], donor atoms in silicon [45], quantum Hall systems [46], and electrons on helium [47].

Moreover, we have experimentally demonstrated the present scheme for obtaining a two-qubit state from the results of repeated measurements with a single, factorized observable, where another two-qubit system is introduced as the assistant. We performed the experiments for the three different initial states: the equilibrium state $\hat{\rho}_{S1}$, the pseudo-pure state $\hat{\rho}_{S2}$, and the pseudo-entangled state $\hat{\rho}_{S3}$. After an evolution under a designed pairwise interaction, we measured the x components of the whole system $S + A$. The joint probabilities give the initial density matrix of the system S by a one-to-one mapping. The experimental results are good agreement with the theoretical exceptions. In our NMR experiments, measuring a single observable leads to a simpler reading-out procedure, since only x components are required. As a price, this method requires an assistant with the same dimension and a nontrivial system-assistant interaction. Therefore, the single-apparatus quantum state tomography is important for a situation with a physically transparent measurement base and with a realistic system-assistant interaction. We hope this practical QST with a single observable will be useful in large-qubit systems.

ACKNOWLEDGMENTS

The authors thanks Prof. S. J. Wu for the useful discussion. This work is supported by the National Key Basic Research Program of China (Grants No. 2013CB921800 and No. 2014CB848700), the National Natural Science Foundation of China under Grants No. 11375167, No. 11227901, and No. 91021005, the Chinese Academy Of Sciences, the Strategic Priority Research Program (B) of the CAS (Grant No. XDB01030400), the Research Fund for the Doctoral Program of Higher Education of China under Grant No. 20113402110044, and the Scientific Research Foundation for the Returned Overseas Chinese Scholars, State Education Ministry.

[1] C. W. Helstrom, *Quantum Detection and Estimation Theory* (Academic, New York, 1976).
[2] D. F. V. James, P. G. Kwiat, W. J. Munro, and A. G. White, Phys. Rev. A **64**, 052312 (2001).
[3] R. T. Thew, K. Nemoto, A. G. White, and W. J. Munro, Phys. Rev. A **66**, 012303 (2002).
[4] A. E. Allahverdyan, R. Balian, and Th. M. Nieuwenhuizen, Phys. Rev. Lett. **92**, 120402 (2004).
[5] X. Peng, J. Du, and D. Suter, Phys. Rev. A **76**, 042117 (2007).
[6] Y. Yu, H. Wen, H. Li, and X. Peng, Phys. Rev. A **83**, 032318 (2011).
[7] A. Shukla, K. R. K. Rao, and T. S. Mahesh, Phys. Rev. A **87**, 062317 (2013).
[8] E. Prugovečki, Int. J. Theor. Phys. **16**, 321 (1977).
[9] S. T. Flammia, A. Silberfarb, and C. Caves, Found. Phys. **35**, 1985 (2005).
[10] J. M. Renes, R. Blume-Kohout, A. J. Scott, and C. M. Caves, J. Math. Phys. **45**, 2171 (2004).
[11] T. Durt, C. Kurtsiefer, A. Lamas-Linares, and A. Ling, Phys. Rev. A **78**, 042338 (2008).
[12] R. Salazar, D. Goyeneche, A. Delgado, and C. Saavedra, Phys. Lett. A **376**, 325 (2012).
[13] R. B. A. Adamson and A. M. Steinberg, Phys. Rev. Lett. **105**, 030406 (2010).
[14] A. B. Klimov, C. Muñoz, A. Fernández, and C. Saavedra, Phys. Rev. A **77**, 060303 (2008).
[15] G. Lima, L. Neves, R. Guzmán, E. S. Gómez, W. A. T. Nogueira, A. Delgado, A. Vargas, and C. Saavedra, Opt. Express **19**, 3542 (2011).
[16] R. Salazar and A. Delgado, Phys. Rev. A **86**, 012118 (2012).
[17] J. S. Lundeen and C. Bamber, Phys. Rev. Lett. **108**, 070402 (2012).
[18] S. Wu, Sci. Rep. **3**, 1193 (2013).
[19] D. Gross, Y. K. Liu, S. T. Flammia, S. Becker, and J. Eisert, Phys. Rev. Lett. **105**, 150401 (2010).
[20] W. T. Liu, T. Zhang, J. Y. Liu, P. X. Chen, and J. M. Yuan, Phys. Rev. Lett. **108**, 170403 (2012).
[21] A. M. Brańczyk, D. H. Mahler, L. A. Rozema, A. Darabi, A. M. Steinberg, and D. F. V. James, New J. Phys. **14**, 085003 (2012).
[22] D. Mogilevtsev, J. Řeháček, and Z. Hradil, New J. Phys. **14**, 095001 (2012).
[23] S. T. Merkel, J. M. Gambetta, J. A. Smolin, S. Poletto, A. D. Córcoles, B. R. Johnson, C. A. Ryan, and M. Steffen, Phys. Rev. A **87**, 062119 (2013).
[24] R. Blume-Kohout, J. K. Gamble, E. Nielsen, J. Mizrahi, J. D. Sterk, and P. Maunz, arXiv:1310.4492.
[25] M. Takahashi, S. D. Bartlett, and A. C. Doherty, Phys. Rev. A **88**, 022120 (2013).
[26] N. Bohr, Phys. Rev. **48**, 696 (1935).
[27] B. Mehmani, A. E. Allahverdyan, and Th. M. Nieuwenhuizen, Phys. Rev. A **77**, 032122 (2008).
[28] B. Mehmani and Th. M. Nieuwenhuizen, J. Comput. Theor. Nanosci. **8**, 937 (2011).
[29] G. M. D'Ariano, Phys. Lett. A **300**, 1 (2002).
[30] D. G. Cory, A. F. Fahmy, and T. F. Havel, Proc. Natl. Acad, Sci. USA **94**, 1634 (1997).
[31] N. A. Gershenfeld and I. L. Chuang, Science **275**, 350 (1997).
[32] J. S. Lee, Phys. Lett. A **305**, 349 (2002).
[33] E. M. Fortunato, M. A. Pravia, N. Boulant, G. Teklemariam, T. F. Havel, and D. G. Cory, J. Chem. Phys. **116**, 7599 (2002).
[34] D. G. Cory, M. D. Price, and T. F. Havel, Physica D: Nonlin. Phenom. **120**, 82 (1998).
[35] L. M. K. Vandersypen and I. L. Chuang, Rev. Mod. Phys. **76**, 1037 (2005).
[36] H. Trotter, Proc. Am. Math. Soc. **10**, 545 (1959).
[37] M. A. Nielsen and I. L. Chuang, *Quantum Computation and Quantum Information* (Cambridge University Press, Cambridge, 2000).
[38] D. Lu, N. Xu, R. Xu, H. Chen, J. Gong, X. Peng, and J. Du, Phys. Rev. Lett. **107**, 020501 (2011).
[39] N. Xu, J. Zhu, D. Lu, X. Zhou, X. Peng, and J. Du, Phys. Rev. Lett. **108**, 130501 (2012).
[40] N. Khaneja, T. Reiss, C. Kehlet, T. Schulte-Herbrüggen, and S. J. Glaser, J. Magn. Reson. **172**, 296 (2005).

[41] M. H. Levitt, *Spin Dynamics: Basics of Nuclear Magnetic Resonance* (John Wiley & Sons, New York, 2008).
[42] S. M. Reimann and M. Manninen, Rev. Mod. Phys. **74**, 1283 (2002).
[43] P. Xue, Phys. Rev. A **81**, 052331 (2010).
[44] M. Trif, V. N. Golovach, and D. Loss, Phys. Rev. B **75**, 085307 (2007).
[45] H. Mirzaei and H. T. Hui, J. Appl. Phys **108**, 094503 (2010).
[46] T. Chakraborty, Adv. Phys. **49**, 959 (2000).
[47] P. M. Platzman and M. I. Dykman, Science **284**, 1967 (1999).